not further affect the anisotropy of the tensor, although it does reduce the asymmetry parameter. The τ tensor is largely unaffected by these events, in accord with a picture of poor communication between the ring nitrogens in the solid. In the solid state, only a single tautomeric species is detected for each of the protonation states, in contrast to the mixture of tautomers found in solution. The predominant tautomer found in solution, however, is the one also observed in the solid state. The isotropic chemical shift values can be used to interpret the solution chemical shifts in terms of the tautomeric equilibria, and the results agree reasonably well with the analysis based on coupling constants in solution. We anticipate that the methods used here will permit a similar analysis to be made of the state of histidine in a large system, such as a protein.

Acknowledgment. This research was supported by the National Institutes of Health (GM-23403, GM-27927, GM-23316, GM-26272, and RR-00995) and by the National Science Foundation (C-670). J.H. is supported by a Faculty Research Award from the American Cancer Society. Thanks are accorded to Drs. W. P. Aue and T. H. Huang for their assistance and advice.

Registry No. L-Histidine, 71-00-1; DL-histidine, 4998-57-6; imidazole, 288-32-4; L-histidine cation, 70805-60-6; L-histidine anion, 26302-81-8; DL-histidine cation, 80448-36-8; DL-histidine anion, 80448-37-9.

Origins of Inhomogeneous Broadening in the Vibronic Spectra of Visual Chromophores and Visual Pigments

Robert R. Birge,* David F. Bocian, and Lynn M. Hubbard[1]

Contribution from the Department of Chemistry, University of California, Riverside, California 92521. *Received May 1, 1981*

Abstract: The origins of inhomogeneous broadening in the vibronic spectra of visual chromophores and pigments are analyzed using the INDO-PSDCI molecular orbital theory and the expansion of selected coordinate potential functions in a generalized anharmonic basis set. Our analysis differentiates between two mechanisms of inhomogeneous broadening: "horizontal" and "vertical". Horizontal inhomogeneity is described in terms of a distributed coordinate effect, whereas vertical inhomogeneity is described in terms of a $\pi^* \leftarrow \pi$ vibronic effect. The primary source of inhomogeneous broadening in the ambient temperature electronic absorption spectra of the retinal isomers in solution is horizontal inhomogeneity in the C_6–C_7 torsional coordinate. Our results are therefore in general agreement with the previous literature on this subject. However, our calculations indicate that at 1.8 K, the C_6–C_7 torsional angle of *all-trans*-retinal is restricted to a relatively small range of dihedral angles ($\phi_{6,7}$ = 52.4 ± 4°). The primary source of broadening of the principal absorption bands of the visual chromophores at very low temperatures is shown to be vertical inhomogeneity associated with the C_6–C_7 torsional potential surface. The λ_{max} absorption bands of the pigments, rhodopsin and bacteriorhodopsin, are predicted to be broadened by vertical inhomogeneity associated with one or more barrierless excited state potential surface(s) for double-bond isomerization. In particular, the C_{11}=C_{12} torsional surface in the lowest $\pi\pi^*$ state of the 11-cis chromophore is sufficient unto itself for producing spectral diffuseness in the λ_{max} band of rhodopsin down to 1.8 K. The C_6–C_7 torsional potential surface is predicted to be a minor source of inhomogeneous broadening in rhodopsin and bacteriorhodopsin. We conclude that the mechanism of spectral broadening in the isolated chromophores is distinctly different from that responsible for spectral broadening in the visual and bacterial pigments.

I. Introduction

The low-energy electronic λ_{max} absorption bands of the visual chromophores (Figure 1) and the visual pigments rhodopsin and bacteriohodopsin (Figure 2) are characterized by a total absence of distinct vibronic structure.[2] The λ_{max} absorption bands of the retinal isomers are completely inhomogeneously broadened in low-temperature (77 K) solvent glasses although many of the higher-energy electronic bands display a degree of vibronic development (Figure 1). Furthermore, this inhomogeneous broadening of the retinal λ_{max} band persists at extremely low temperatures (1.8 K) where the Boltzmann population of upper vibrational levels of the ground state is negligible.[3]

Christensen and Kohler were the first investigators to study this phenomenon in detail, and these investigators experimentally demonstrated that torsional freedom around the 6–7 single bond is the essential element in producing spectral diffuseness in retinyl polyenes.[4] A salient experimental demonstration of this effect can be observed in the absorption spectrum of anhydrovitamin A, a molecule with a 6,7 double bond which restricts torsional distortion (Figure 3). Theoretical calculations provide general support for Christensen and Kohler's arguments by predicting that the ground state potential surface of the 6,7 dihedral torsional angle is shallow[5,6] whereas the excited state potential surface is much steeper.[6] Subsequent experimental and theoretical studies have provided additional evidence to support the above interpretation.[7-9] However, a number of important questions remain to be answered. For example, why does the principal absorption band of *all-trans*-retinal remain diffuse at liquid helium temperature?[3] Furthermore, why are the main absorption bands of the visual pigments also diffuse at low temperatures (4–77 K)?[10,11] The above two questions are interesting because they imply a

(1) UCAR graduate student fellow.
(2) Birge, R. R. *Annu. Rev. Biophys. Bioeng.* **1981**, *10*, 315.
(3) The absorption spectrum of *all-trans*-retinal in EPA at 1.8 K (liquid helium) exhibits no enhancement in the vibronic structure of the λ_{max} absorption band over that shown in Figure 1. Auerbach, R. A.; Birge, R. R.; Kohler, B. E.; Sullivan, M. J., unpublished results.
(4) Christensen, R. L.; Kohler, B. E. *Photochem. Photobiol.* **1973**, *18*, 293.
(5) Honig, B.; Hudson, B.; Sykes, B. D.; Karplus, M. *Proc. Natl. Acad. Sci. U.S.A.* **1971**, *68*, 1289.
(6) Warshel, A.; Karplus, M. *J. Am. Chem. Soc.* **1974**, *96*, 5677.
(7) (a) Hemley, R.; Kohler, B. E. *Biophys. J.* **1977**, *20*, 377. (b) Das, P. K.; Becker, R. S. *J. Phys. Chem.* **1978**, *82*, 2081, 2093.
(8) (a) Blatz, P. E.; Dewhurst, P. B.; Balasvbramaniyan, V.; Balasvbramaniyan, P.; Lin, M. *Photochem. Photobiol.* **1970**, *11*, 1. (b) Mao, B.; Govindjee, R.; Ebrey, T. G.; Arnaboldi, M.; Balogh-Nair, V.; Nakanishi, K.; Crouch, R. *Biochemistry* **1981**, *20*, 428.
(9) Honig, B.; Dinur, U.; Birge, R. R.; Ebrey, T. G. *J. Am. Chem. Soc.* **1980**, *102*, 488.
(10) Yoshizawa, T.; Wald, G. *Nature (London)* **1963**, *197*, 1279.
(11) Becher, B.; Tokunaga, F.; Ebrey, T. G. *Biochemistry* **1978**, *17*, 2293.

0002-7863/82/1504-1196$01.25/0

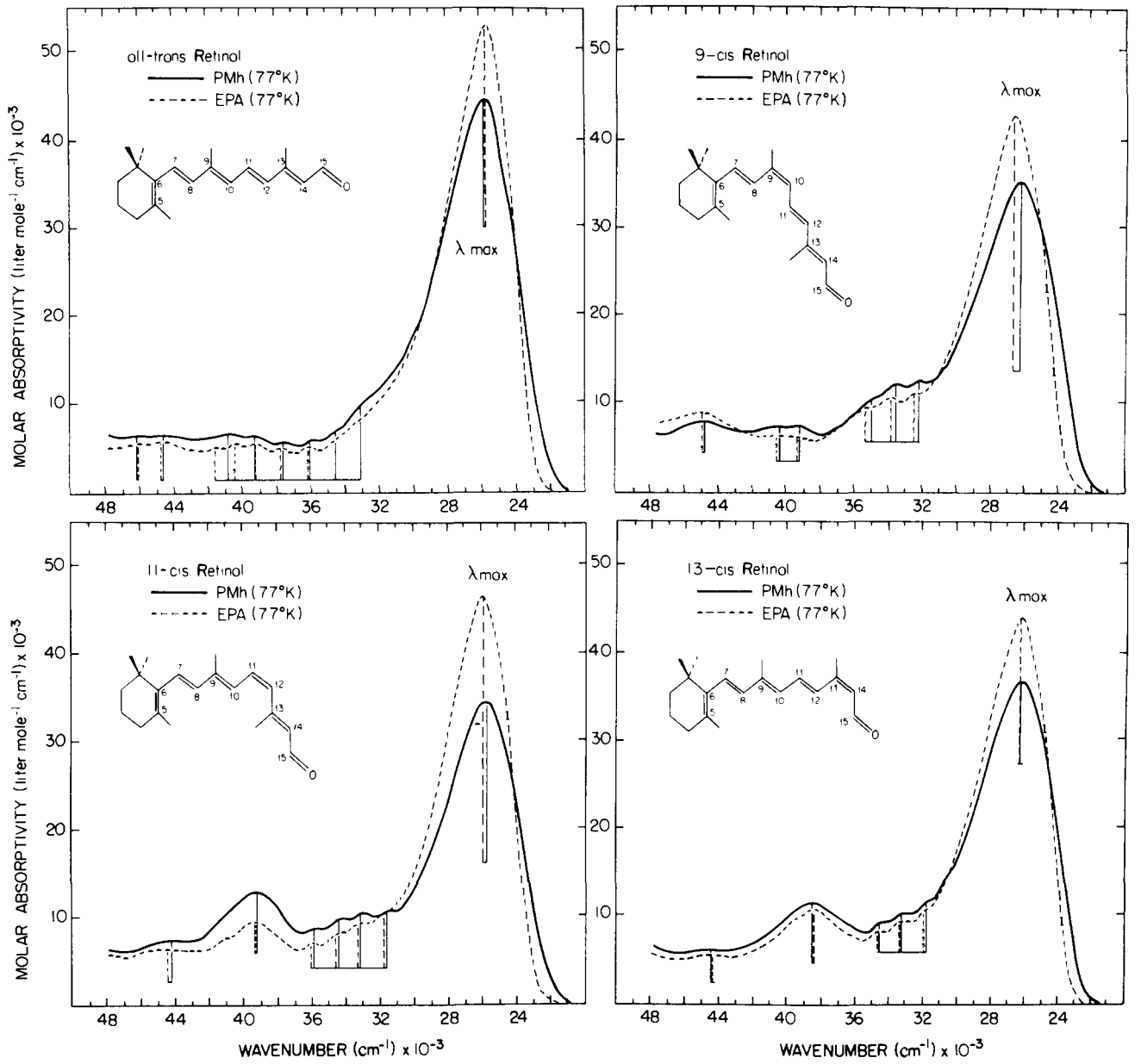

Figure 1. Low-temperature (77 K) absorption spectra of selected retinal isomers in EPA (ethyl ether:isopentane:alcohol; 5:5:2, v/v) and in PMH (isopentane:methylcyclohexane; 5:1; v/v). Note that the λ_{max} absorption bands are broad and unstructured, but that some of the higher energy absorption bands display vibronic structure.

source of inhomogeneous broadening that is more complicated than most of the previous literature on this subject would suggest.

In this paper we report the explicit calculation of the vibrational energy levels for the C_6–C_7 torsion in the ground and excited electronic states of *all-trans*-retinal and the resulting Franck–Condon overlap integrals. An adequate theoretical description of this effect requires the use of a generalized vibrational treatment capable of including anharmonicity in the excited state vibrational manifold. We calculate the following ground state vibrational energy levels for the C_6–C_7 torsional degree of freedom in *all-trans*-retinal: 11.6 cm^{-1} (0), 32.5 cm^{-1} (1), 51.4 cm^{-1} (2), 70.2 cm^{-1} (3), etc. Each of these levels is doubly degenerate and at 1.8 K, >99% of the molecules occupy the zero-point level (11.6 cm^{-1}). Accordingly, the argument that inhomogeneity in the ground state C_6–C_7 torsional angle is responsible for the spectra diffuseness becomes suspect. We will demonstrate that the range of C_6–C_7 dihedral angles occupied by *all-trans*-retinal in the $v = 0$ level is small (77% of the molecules are in the range 52.4 ± 4°). Thus, the source of the spectral diffuseness at low temperatures is primarily vibronic in nature.

The question of why the visual pigments display spectral diffuseness is interesting because the protein environment will significantly decrease the importance of the β-ionylidene ring torsion in generating diffuseness. Binding experiments suggest that the β-ionylidene ring is trapped in a hydrophobic cleft in the binding site of opsin.[12,13] Although the binding site displays a surprising degree of "lenience",[14] the existence of a binding site even slightly stereospecific to the β-ionylidene ring will drastically alter the ground and excited state potential surfaces for C_6–C_7 dihedral motion. A degree of conformational restraint will be introduced that will generate a deeper potential well in the ground state and decrease the coordinate inhomogeneity in the torsional degree of freedom. Furthermore, the fact that the conformational constraint is external will force the ground and excited state dihedral angle minima to be similar. The importance of vibronic effects to spectral broadening will therefore decrease. Of equal, or greater, importance is the observation that the chromophores in rhodopsin and bacteriorhodopsin are bound to the proteins via protonated

(12) Blatz, P. E.; Lin, M.; Balasvbramanigan, P.; Balasvbramanigan, V.; Bewhurst, P. B. *J. Am. Chem. Soc.* **1969**, *91*, 5930.
(13) Matsumoto, H.; Yoshizawa, T. *Nature (London)* **1974**, *258*, 523.
(14) Blatchly, R. A.; Carriker, J. D.; Balogh-Nair, V.; Nakanishi, K. *J. Am. Chem. Soc.* **1980**, *102*, 2495.

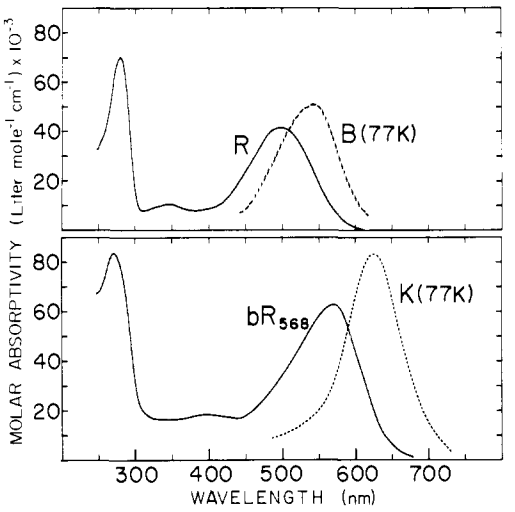

Figure 2. Absorption spectra of rhodopsin at room temperature (R), bathorhodopsin at 77 K [B(77K)], the light-adapted form of bacteriorhodopsin at room temperature (bR_{568}), and the K_{610} intermediate at 77K [K(77K)]. The figure is adapted from ref 2. The λ_{max} bands of rhodopsin (R) and bR_{568} remain broad and unstructured at all temperatures investigated (1.8–300 K).

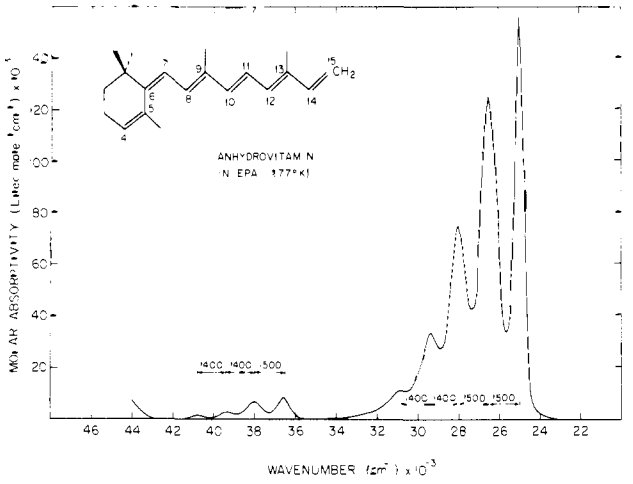

Figure 3. Low-temperature absorption spectrum of anhydrovitamin A in EPA (77 K). The spectrum was taken by Professor R. L. Christensen.

Schiff base linkages.[2,15] The extensive charge redistribution that occurs upon replacing the carbonyl oxygen with a protonated nitrogen atom decreases the extent of polyene bond order alternation.[16,17] Furthermore, excitation into the lowest "$^1B_u^{*+}$" $\pi\pi^*$ state induces a significant reorganization of electron density toward nitrogen.[18] These two effects decrease the extent of C_6–C_7 bond order reversal upon excitation.[16] For example, INDO-PSDCI[19] calculations on *all-trans*-retinal predict a 38% increase in the C_6–C_7 bond order upon excitation. In contrast, the protonated Schiff base of *all-trans*-retial is calculated to have only a 20% increase in the C_6–C_7 bond order upon excitation. A negatively charged counterion near the nitrogen atom lowers the above percent increase to 8–18% depending upon location. The calculations suggest, therefore, that C_6–C_7 torsional effects should be of significantly less importance in producing spectral diffuseness in the electronic spectra of the protonated Schiff bases of retinal. Experimental evidence in support of this prediction can be found in the spectroscopic data of Waddell, Schaffer, and Becker.[20] These authors observed sharp vibronic structure in the low temperature (77 K) λ_{max} absorption bands of the *all-trans*- and 11-*cis*-retinal protonated Schiff bases after bubbling anhydrous HCl through the solutions. Presumably, the excess HCl acts to produce a local counterion cage which produces λ_{max} values very similar to those observed in the pigments.[20]

The above arguments, and the observation that the λ_{max} absorption bands of artificial pigments formed from 5,6-dihydroretinal are broad and unstructured,[8] suggest that β-ionylidene ring torsion is not the primary source of spectral diffuseness in the visual pigments. We demonstrate in this paper that the primary source may be a manifestation of a barrierless excited state potential surface for double-bond isomerization. Explicit calculation of the energy levels for the C_{11}=C_{12} torsion in the ground and $\pi\pi^*$ excited states and the resulting Franck–Condon overlap integrals indicates that the vibronic activity of the C_{11}=C_{12} excited state torsional mode of the protein bound chromophore in rhodopsin is sufficient unto itself to induce spectral diffuseness down to 1.8 K.

II. Theoretical

A. Potential Surface Calculations. The ground state potential surface for the C_6–C_7 torsional degree of freedom was calculated using standard INDO-SCF procedures[21] with partial adiabatic minimization of other selected conformational degrees of freedom using gradient procedures.[22] The entire molecular framework was included. The following degrees of freedom were iteratively adjusted to yield the lowest energy conformation as a function of selected C_6–C_7 dihedral angles: $R_{6\text{-}7}$; $R_{7\text{-}8}$; $R_{8\text{-}9}$; $R_{9\text{-}10}$; θ(5–6–7); θ(6–7–8); θ(7–8–9); θ(8–9–10); Φ(6–7–8–9); Φ(7–8–9–10); Φ(9–10–11–12); $\Phi(C_1\text{–}CH_3$; both); $\Phi(C_5\text{–}CH_3)$; $\Phi(C_9\text{–}CH_3)$, where R, θ, and Φ represent bond length, bond angle, and dihedral angle and $\Phi(C_i\text{–}CH_3)$ indicates a methyl torsion for the methyl group attached to atom i. The remaining internal coordinates were held fixed at the crystal geometry values.[23] Accordingly, the C_6–C_7 potential surface is only partially adiabatically minimized. This limitation, along with those inherent in the use of the semiempirical molecular orbital INDO-SCF formulation, precludes our surface from being rigorously accurate. Nevertheless, it is sufficiently accurate for the purposes of our vibrational analysis.

The potential surface for the C_6–C_7 dihedral angle was calculated by carrying out the above minimization in 15° increments from 0° to −180°. These data points were converted to a smaller grid of 2.5° increments using five point Lagrangian interpolation assuming the surface from 0° to 180° is a "mirror image" of that calculated from 0° to −180°. This is not rigorously correct, but is of no importance to the present vibrational analysis (see below). The final surface is shown at the bottom of Figure 4. The potential surface minimum is calculated to be a 6-s-cis (−51.7°), in reasonable agreement with the crystal structure data[22] [6-s-cis (−58.3°)]. A second minimum at 6-s-trans (180°) is calculated to be 1497 cm^{-1} above the 6-s-cis (−51.7°) minimum. Assuming our surface is representative of the C_6–C_7 torsional potential surface in solution, >99% of the molecules in solution will have a 6-s-cis conformation. Our ground state C_6–C_7 potential surface is in essential agreement with previous theoretical[5,6,23-25] and experimental[5,25,26] investigations.

The excited state C_6–C_7 torsional potential surfaces were calcualted using the INDO-PSDCI molecular orbital theory.[18,19,27]

(15) Oseroff, A.; Callender, R. *Biochemistry* **1974**, *13*, 4243.
(16) Leclercq, J. M.; Sandorfy, C. *Photochem. Photobiol.* **1981**, *33*, 361.
(17) Schulten, K.; Dinur, U.; Honig, B. *J. Chem. Phys.* **1980**, *73*, 3927.
(18) Birge, R. R.; Hubbard, L. M. *J. Am. Chem. Soc.* **1980**, *102*, 2195.
(19) "INDO-PSDCI" stands for Intermediate Neglect of Differential Overlap including Partial Single and Double excitation Configuration Interaction. We previously used the acronym INDO-CISD to signify these procedures (ref 18). One referee, however, noted that "CISD" normally signifies complete single and double CI; hence our use of "INDO-PSDCI" in the present paper.
(20) Waddell, W. H.; Schaffer, A. M.; Becker, R. S. *J. Am. Chem. Soc.* **1977**, *99*, 8456.
(21) Pople, J. A.; Segal, G. A. *J. Chem. Phys.* **1976**, *44*, 3289.
(22) McIver, J. W., Jr.; Komornicki, A. *Chem. Phys. Lett.* **1971**, *10*, 303.
(23) Hamanaka, T.; Mitsui, T.; Ashida, T.; Kakudo, M. *Acta Crystallogr., Sect. B* **1972**, *28*, 214.
(24) Pullman, B.; Langlet, J.; Berthod, H. *J. Theor. Biol.* **1969**, *23*, 492.
(25) Rowan, R.; Warshel, A.; Sykes, B. D.; Karplus, M. *Biochemistry* **1974**, *13*, 970.
(26) Becker, R. S.; Berger, S.; Dalling, D. K.; Grant, D. M.; Pugmire, R. J. *J. Am. Chem. Soc.* **1974**, *96*, 7008.

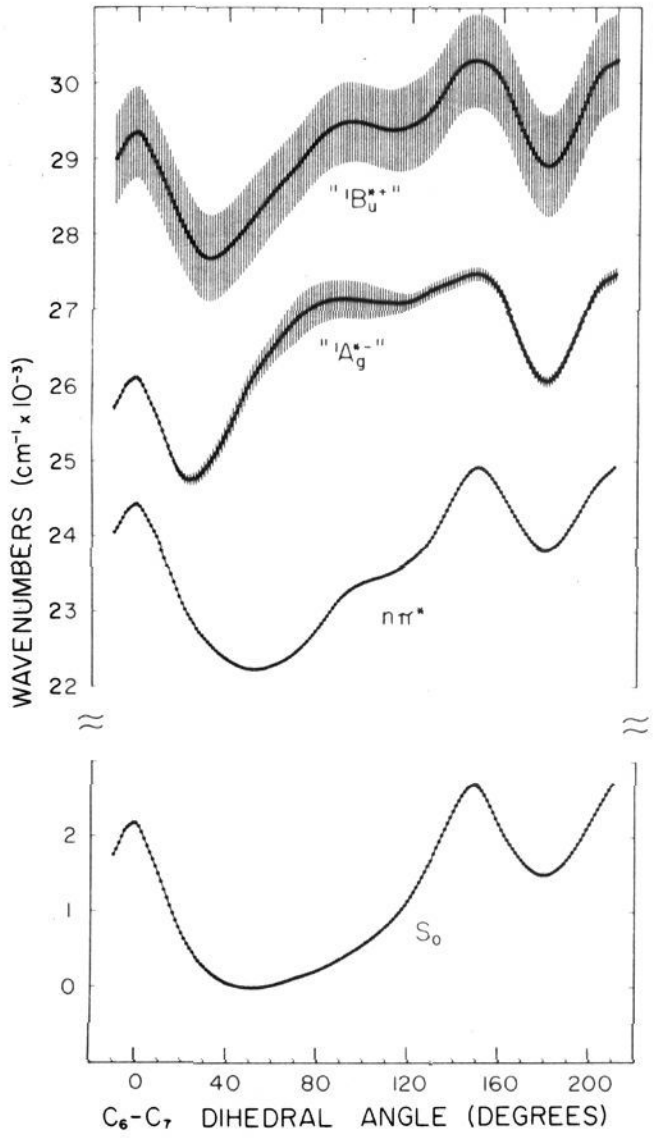

Figure 4. Ground and low-lying excited singlet state potential surfaces for the C_6–C_7 torsional degree of freedom in *all-trans*-retinal. The ground-state surface was calculated using the INDO-SCF procedures with partial adiabatic minimization (see text). The excited-state surfaces were calculated using the INDO-CISD procedures. The $n\pi^*$ state surface has been plotted 6000 cm^{-1} below its calculated position (cf., Figure 5) to facilitate comparison. The vertical lines superimposed on the "$^1A_g^{*-}$" and "$^1B_u^{*+}$" state potential surfaces are proportional to the oscillator strength of the electron transition from the ground state as a function of C_6–C_7 dihedral angle. The "$^1A_g^{*-}$" state oscillator strength lines are multiplied by three relative to those of the "$^1B_u^{*+}$" state to improve visibility.

The "truncated" chromophore shown below was used to represent the retinal polyene system

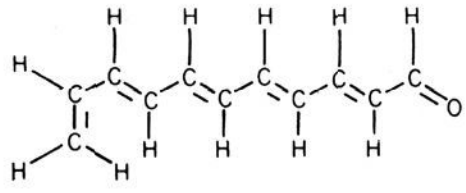

All single excitations below 13 eV (~150), and a selected number of the lowest energy double excitations determined using the ratio formula described in ref 18 (~300), were included in the CI Hamiltonian. These calculations yielded the transition energies and oscillator strengths for selected C_6–C_7 dihedral angles. The results are shown in Figure 5. The transition energies were then added to the ground state potential surface to generate the excited state potential surfaces shown in Figure 4. (Note that the $n\pi^*$ surface has been linearly shifted 6000 cm^{-1} below its calculated position to facilitate visual comparisons of the three surfaces.)

Our approach to the calculation of the excited state surfaces is approximate because we have not carried out adiabatic minimization of each surface independently. Before we examine the errors inherent in our approach, we should note the reasons for adopting the above approximate procedures. A single INDO-PSCDI calculation on the truncated chromophore shown above using a CI basis set of ~150 singles and ~300 doubles takes ~18 min of CPU time on a Cray computer (4×10^7 floating point operations per second). We estimate that it would take at least 20 times the above CPU time to minimize the energy for a single excited state. Furthermore, the results would not be meaningful because the truncated chromophore lacks the methyl groups and β-ionylidene ring of the retinal chromophore. Furthermore, we do not believe our approach will introduce serious error. A comparison of the "$^1B_u^{*+}$" excited state surface with the analogous surface calculating using semiempirical π-electron consistent force field (QCFF) procedures (ref 6) indicates that both methods yield very similar results. Our calculation predicts a C_6–C_7 "$^1B_u^{*+}$" dihedral angle minimum at −32.3°; the QCFF calculation predicts −33° (Table II of ref 6). We do expect that our approximate approach will overestimate the excited state barriers of 6-s-cis to 6-s-trans torsional interconversion. This error will tend to increase the vibronic level spacing, and decrease the anharmonicity, of the higher energy vibronic manifold in the excited state. As one referee correctly noted, this will lead to overestimations of the Franck–Condon factors for individual vibronic levels. However, the net effect on the entire vibronic envelope is unlikely to be significant. We firmly believe that the excited state surfaces are sufficiently accurate for the purposes of the present study of vibronically induced spectral broadening.

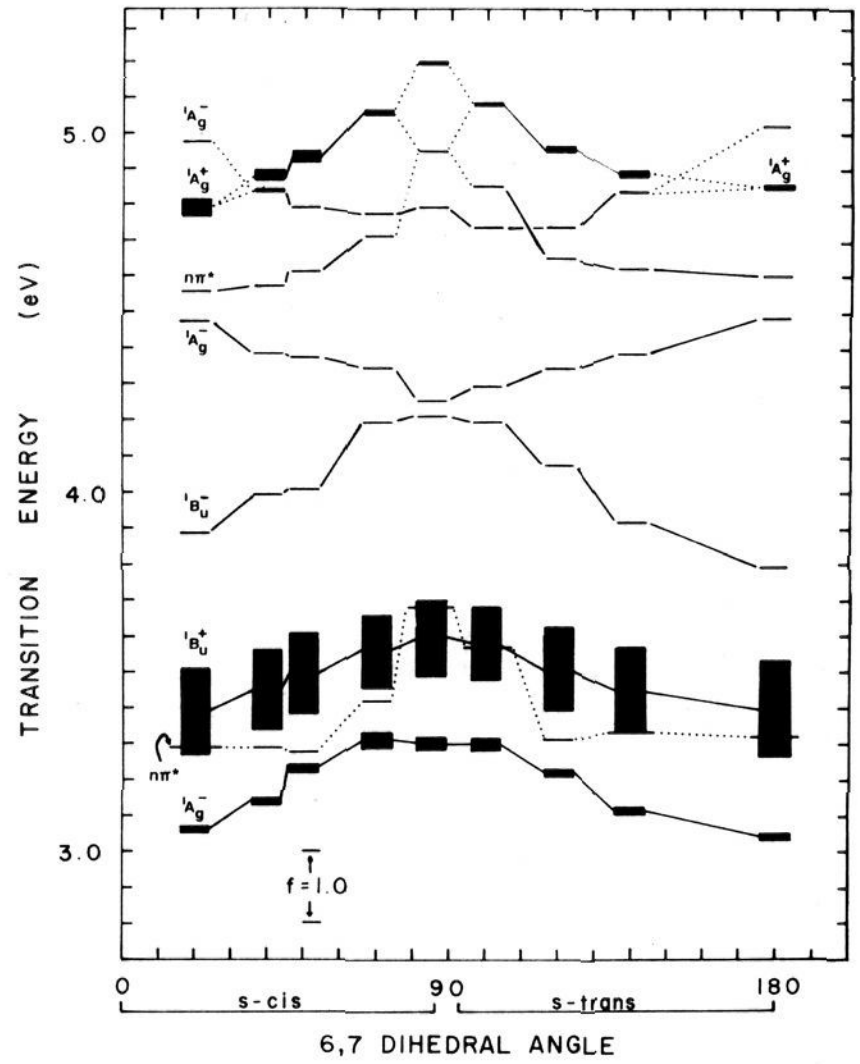

Figure 5. INDO-CISD transition energies and oscillator strengths in *all-trans*-retinal as a function of the C_6–C_7 dihedral angle. The individual states are indicated by rectangular boxes and the height is proportional to the oscillator strength. The symmetry labels are approximate and significant state mixing occurs in the higher energy manifold.

The ground and excited state potential surfaces associated with the C_{11}=C_{12} [Φ(10,11,12,13)] dihedral angle were taken from ref 18 and were generated using INDO-PSDCI[19] procedures. The calculational details are described in ref 18. It proved necessary to slightly smooth the excited state surface prior to Fourier transformation (see section II.B.1). Minor discontinuities in the surface generated using the INDO-PSDCI procedures prevented an accurate representation of the surface using a reasonable number of Fourier expansion coefficients.

B. Vibronic Analysis. The energy levels for the torsional vibrations about the C_6–C_7 and C_{11}=C_{12} bonds in both the ground and excited electronic states were calculated under the assumption that the particular torsional oscillation was separable from all the

(27) Hubbard, L. M. Ph.D. Thesis, University of California, Riverside, CA, 1981.

other vibrations of the molecule. This represents the most severe approximation inherent in our analysis and the consequences are discussed in detail in section III.A.3. The vibrational coordinate for the torsional motion is then defined by the dihedral angle Φ_{ijkl} ($\Phi_{5,6,7,8}$ or $\Phi_{10,11,12,13}$), although certain other internal coordinates of the molecule change as a function of changes in the principal coordinate (see above). The Hamiltonian for the torsional motion is then given by

$$\mathcal{H} = BP_\Phi^2 + V(\Phi) \quad (1)$$

where $V(\Phi)$ is the potential energy as a function of the dihedral angle, Φ, and B is the kinetic energy function for the torsional oscillation.

1. Fourier Transformation of the Potential Energy Surfaces. The potential energy as a function of the dihedral angle about the C_6–C_7 and C_{11}=C_{12} bonds in both the ground and excited electronic states is assumed to be symmetric about 0° (see section II.A). Consequently, the potential function $V(\Phi)$ is conveniently expressed as a Fourier cosine series

$$V(\Phi) = V_0 + V_1 \cos(\Phi) + V_2 \cos(2\Phi) + V_3 \cos(3\Phi) + \ldots + V_n \cos(n\Phi) \quad (2)$$

The coefficients, V_n, can be obtained for a given potential function by taking the Fourier transform of the potential curve. The expansion coefficients are given by the expressions

$$V_0 = (1/N)\sum_{i=1}^{N} V(\Phi_i) \quad (3a)$$

$$V_n = (2/N)\sum_{i=1}^{N} V(\Phi_i) \cos(n\Phi_i) \quad (3b)$$

where N is the number of data points used in the transform. The expansion coefficients for the potential functions for the torsions about the C_6–C_7 and C_{11}=C_{12} bonds were calculated by evaluating the potential energy at 2.5° intervals between 0° and 360° and then taking a 144-point Fourier transform using eq 3. The coefficients for n up to 25 were calculated for the four potential surfaces. The potential energy expansions for all the torsional vibrations are dominated by terms $V_n < 10$, but higher order coefficients also make significant contributions to the expressions. The calculations of the energy levels for each of the potential surfaces used 25 term expansions.

2. Calculation of the Kinetic Energy. The inverse of the kinetic energy function of the one-dimensional Hamiltonian given by eq 1 can be expressed as

$$B^{-1} = \sum_k m_k[\partial \hat{r}_k/\partial\Phi]^2 \quad (4)$$

where m_k and $\hat{r}_k$ are the mass and cartesian coordinate vector of the kth atom, respectively. For obtaining the vibrational kinetic energy free from contributions due to translational and rotational motions, values of $\partial \hat{r}_k/\partial\Phi$ must be obtained which satisfy the two conditions

$$\sum_k m_k[\partial \hat{r}_k/\partial\Phi] = 0 \quad (5a)$$

$$\sum_k m_k \hat{r}_k \times [\partial \hat{r}_k/\partial\Phi] = 0 \quad (5b)$$

Condition 5a is satisfied by referring the coordinate vectors to the center of mass of the molecule. Condition 5b can be satisfied by applying the transformation given by Eckart (see, for example, ref 28a) which results in the expression for the kinetic energy

$$B^{-1} = \sum_k m_k[\partial \hat{r}_k/\partial\Phi]^2 - \sum_i\sum_j\sum_k m_k\{[\hat{r}_k \times (\partial \hat{r}_k/\partial\Phi)]_i I_{ij}^{-1}[\hat{r}_k \times (\partial \hat{r}_k/\partial\Phi)]_j\} \quad (6)$$

where I_{ij}^{-1} is the ij inverse element of the inertial tensor for the molecule.

The kinetic energies for the torsions about the C_6–C_7 and C_{11}=C_{12} bonds were calculated using eq 6. The derivatives were evaluated numerically with a value of $\Delta\Phi$ equal to 0.01°. The values of B calculated for the torsion about the C_{11}=C_{12} bond vary somewhat as a function of the dihedral angle. The maximum value of B (0.179 cm^{-1}) is obtained for the motion when the molecule is in the 11-cis conformation and the minimum value (0.151 cm^{-1}) is obtained for the all-trans conformer. We arbitrarily used the value of B obtained for the 11-cis conformation in our calculation of the energy levels for the torsion about the C_{11}=C_{12} bond because the 11-cis conformation is present in rhodopsin. The calculation of the energy levels using the minimum value of B results in a reduction between the splittings in the energy levels by about 10% (on the average). The use of the smaller B value does not, however, alter the basic pattern of the energy levels nor does it significantly affect the general features of the vibronic spectrum. It should be noted that the variation in the kinetic energy as a function of the torsional angle can be explicitly included in the vibrational Hamiltonian by expanding B in a Fourier series in the torsional angle. Such a detailed treatment of the kinetic energy function is not warranted here, however, since the corrections to the energy levels which would result are probably smaller than the errors which result from our assumption of separability of the torsional vibrations.

The kinetic energy for the torsion about the C_6–C_7 bond was calculated in a manner identical with that described above. The B values for this motion were obtained at various values of the C_6–C_7 dihedral angle with the molecule in the all-trans conformation. The B value calculated for the torsion about the C_6–C_7 bond is ~0.065 cm^{-1} and varies by only ±10% over a full rotation about the bond. A value of B equal to 0.065 cm^{-1} was used in the calculation of the energy levels for this motion.

3. Calculation of the Energy Levels. The energy levels for the various torsional vibrations were calculated by expanding the Hamiltonian of eq 1 in a basis set of a free internal rotor. This basis set can be expressed as either

$$\Psi_m(\Phi) = (2\pi)^{-1/2} e^{im\Phi} \quad (7)$$

$$m = 0, \pm1, \pm2, \pm3, \ldots$$

or

$$\Psi_m(\Phi) = (\pi^{-1/2}) \cos(m\Phi) \quad (8a)$$

$$\Psi_m(\Phi) = (\pi^{-1/2}) \sin(m\Phi) \quad (8b)$$

$$\Psi_0(\Phi) = (2\pi)^{-1/2} \quad (8c)$$

$$m = 1, 2, 3, \ldots$$

The trigonometric basis set (eq 8) preserves the even and odd symmetry in Φ and allows separation of the Hamiltonian into two submatrices of sines and cosines. This latter basis set was used in all of our calculations. The Hamiltonian was diagonalized using a least-squares optimized threshold method.[28b]

The energy levels for the torsional vibrations were initially calculated in a basis set of 81 sin–cos pairs. The Hamiltonian for each mode was rediagonalized in basis sets of 87 and 94 sin–cos pairs to test for convergence of the eigenvalues. It was found that for both the C_6–C_7 and C_{11}=C_{12} torsions in the ground electronic state the levels with substantial population at room temperature (those with energies less than 500 cm^{-1} above the lowest level) had converged to within 0.5 cm^{-1} of their minimum value when the largest basis set was used. The potential well for the C_{11}=C_{12} torsion has a fairly large radius of curvature near the minimum and only three vibrational levels occur at energies less than 500 cm^{-1} above the lowest level. On the other hand, the potential well for the C_6–C_7 torsion is extremely broad and shallow and this combined with the small value of B results in 25 levels with energies less than 500 cm^{-1}. The potential wells for both of the torsional modes in the excited electronic state have much larger radii of curvature than do the respective wells in the ground electronic state. It was found that for both of the excited state potentials wells the lowest 10 energy levels had converged to within

(28) (a) Pickett, H. M. *J. Chem. Phys.* **1972**, *56*, 1715. (b) Birge, R. R.; Hubbard, L. M. *J. Comput. Phys.* **1978**, ,*29*, 199.

3 cm^{-1} of their minimum value when the 94-function basis set was used, and the 50th energy level had converged to within 60 cm^{-1} of its minimum value. The lowest 10 energy levels occur at energies less than 1250 cm^{-1} above the lowest level for the C_{11}=C_{12} torsion and less than 550 cm^{-1} for the C_6–C_7 torsion. The 50th level is ~3500 cm^{-1} above the lowest level in the former potential well and ~2000 cm^{-1} in the latter. The 94-function basis set was used in all of our calculations of the vibronic spectra since reasonable convergence was obtained for the lowest 50 eigenvalues.

4. Calculation of the Franck–Condon Factors. The Franck–Condon factors used to evaluate the vibronic contribution to the electronic absorption spectrum by the C_6–C_7 and C_{11}=C_{12} torsional modes were calculated by taking the direct products of the ground and excited state vibrational eigenfunctions obtained from the diagonalization of the 94-function basis set. The general expression for the even and odd functions is

$$|\Psi_i^{ev}\rangle = \sum_n a_{in} \cos(n\Phi) \tag{9a}$$

$$|\Psi_i^{od}\rangle = \sum_n b_{in} \sin(n\Phi) \tag{9b}$$

The free internal rotation basis set used in the calculations contains the full symmetry for the torsional potential wells of the ground and excited electronic states. Consequently, there is no overlap between even and odd wave functions of the ground and excited states. The nonzero Franck–Condon factors are

$$\langle g_i^{ev}|e_j^{ev}\rangle = \sum_n \sum_m a_{in}^g a_{jm}^e \langle \cos(n\Phi)|\cos(m\Phi)\rangle \delta_{nm} \tag{10a}$$

$$\langle g_i^{od}|e_j^{od}\rangle = \sum_n \sum_m b_{in}^g b_{jm}^e \langle \sin(n\Phi)|\sin(m\Phi)\rangle \delta_{nm} \tag{10b}$$

In eq 10 the terms where $n \neq m$ vanish because of the orthogonality of the free internal rotor basis functions. Thus the Franck–Condon factors are given by

$$\langle g_i^{ev}|e_j^{ev}\rangle = (\text{constant}) \sum_n a_{in}^g a_{jn}^e \tag{11a}$$

$$\langle g_i^{od}|e_j^{od}\rangle = (\text{constant}) \sum_n b_{in}^g b_{jn}^e \tag{11b}$$

The vibronic "stick" spectra were constructed by evaluating $|\langle g_i^{ev}|e_j^{ev}\rangle|^2$ and $|\langle g_i^{od}|e_j^{od}\rangle|^2$ weighted by the appropriate Boltzmann factor. The four lowest vibrational energy levels for the ground electronic state were included in the calculation for the C_{11}=C_{12} torsion and the lowest 20 levels were included for the C_6–C_7 torsion. The lowest 50 levels of torsional oscillation in the excited electronic state were included in the calculations for both torsional modes. The fact that the levels near the 50th level have not converged to better than 60 cm^{-1} of their minimum value does not substantially alter the appearance of the vibronic spectrum since the excited state levels which make the largest contribution to the spectrum are considerably lower in the well where the convergence is much better.

The expectation values for the torsional angle can be evaluated in a manner similar to that used for the Franck–Condon factors. The expectation value of Φ for the ith vibrational level is given by

$$\langle \Psi_i|\Phi|\Psi_i\rangle = \sum_n \sum_m a_{in} a_{im} \langle \cos(n\Phi)|\Phi|\cos(m\Phi)\rangle \tag{12a}$$

$$\langle \Psi_i|\Phi|\Psi_i\rangle = \sum_n \sum_m b_{in} b_{im} \langle \sin(m\Phi)|\Phi|\sin(m\Phi)\rangle \tag{12b}$$

In these expressions the terms $n = m$ are equal to

$$\left.\begin{matrix}\langle \cos(n\Phi)|\Phi|\cos(n\Phi)\rangle \\ \langle \sin(n\Phi)|\Phi|\sin(n\Phi)\rangle\end{matrix}\right\} = \left[\frac{\Phi^2}{4} \pm \frac{\Phi \sin(2n\Phi)}{4n^2} \pm \frac{\cos(2n\Phi)}{8n}\right]_a^b \tag{13}$$

The solutions to the integrals for the terms where $n \neq m$ are given by

$$\left.\begin{matrix}\langle \cos(n\Phi)|\Phi|\cos(m\Phi)\rangle \\ \langle \sin(n\Phi)|\Phi|\sin(m\Phi)\rangle\end{matrix}\right\} = \frac{1}{2}\left[\frac{\cos(n-m)\Phi}{(n-m)^2} + \frac{\Phi \sin(n-m)\Phi}{n-m} \pm \frac{\cos(n+m)\Phi}{(n+m)^2} \pm \frac{\Phi \sin(n+m)\Phi}{n+m}\right]_a^b \tag{14}$$

The lower sign refers to the sin integrals in eq 13 and 14. The integrations were carried out from $\Phi = 0°$ to $\Phi = 180°$ to determine expectation values for the torsional angle assuming the molecule is "isolated" within the above region. Had we integrated over all angles (0° to 360°), the expectation values for all levels would have equaled 180° which is correct but not instructive.

III. Results and Discussion

For the purpose of qualitative discussion, it is useful to differentiate between two mechanisms of inhomogeneous broadening. The first type, which we call "horizontal inhomogeneity", is associated with a broad asymmetric ground state potential surface with closely spaced vibrational energy levels. At room temperature, the Boltzmann population of the higher vibrational levels will provide a range in the average value of the ground state coordinate. Provided the excited state potential surface is different in shape, or its potential minimum is shifted relative to the ground state surface, the inhomogeneity in the ground state coordinate produces a series of energetically different vibronic transitions which can result in a diffuse band. The second type of inhomogeneous broadening, which we call "vertical inhomogeneity", is associated with an excited state anharmonic potential surface which has a potential surface minimum significantly displaced relative to the ground state potential surface minimum. Vibronic transitions from a single ground state vibrational level have maximum "Franck–Condon overlap" with the higher energy, closely spaced (anharmonic) vibrational levels of the excited state. Spectral broadening typically results because a large number of these levels have Franck–Condon activity which generates a diffuse progression over an extended energy range. Vertical inhomogeneous broadening is therefore a vibronic effect whereas horizontal inhomogeneous broadening is primarily a distributed coordinate effect. At very low temperatures where only the ground state vibrational level is populated, vertical inhomogeneity usually dominates horizontal inhomogeneity, because the latter mechanism requires a population of a large number of ground state vibrational levels. At ambient temperatures, however, both mechanisms may be competitive. We demonstrate below that spectral diffuseness associated with the C_6–C_7 torsional mode in the visual chromophores is primarily horizontal at ambient temperature, but primarily vertical at low temperature (i.e., liquid nitrogen or liquid helium temperatures). A major source of spectral diffuseness in the visual pigments, however, may derive from barrierless excited state potential surfaces for double bond isomerization. The latter generates vertical inhomogeneous broadening and is equally effective at all temperatures.

A. The Visual Chromophores. Christensen and Kohler have experimentally demonstrated that the primary source of spectral broadening in the λ_{max} bands of the visual chromophores (Figure 1) is associated with the β-ionylidene, C_6–C_7 single bond torsional degree of freedom.[4] Molecules such as anhydrovitamin A (Figure 3) which have a C_6=C_7 double bond do not display inhomogeneous broadening.[4] Accordingly, we restrict our discussion to an analysis of the C_6–C_7 torsional mode. We further limit our discussion to the "$^1B_u{}^{*+}$" state C_6–C_7 torsional surface because the "$^1A_g{}^{*-}$" state is calculated to provide only ~10% of the total oscillator strength to the λ_{max} band [at $\Phi_{6,7} = 50°$, f("$^1B_u{}^{*+}$" ← S_0) = 1.108, f("$^1A_g{}^{*-}$" ← S_0) = 0.117, f(total) = 1.225, f(obsd, λ_{max}) = 1.24]. The π^* ← n transition is calculated to have a negligible oscillator strength [$f(\pi^* \leftarrow n) = 0.0002$].

The calculated ground state vibrational energy levels are presented in Table I. The vibrational wave functions for three of the low-lying levels are shown at the bottom of Figure 6. The 1 ← 0 transition in the ground state is calculated to be at 21 cm^{-1} and the vibrational manifold is very anharmonic (the calculated

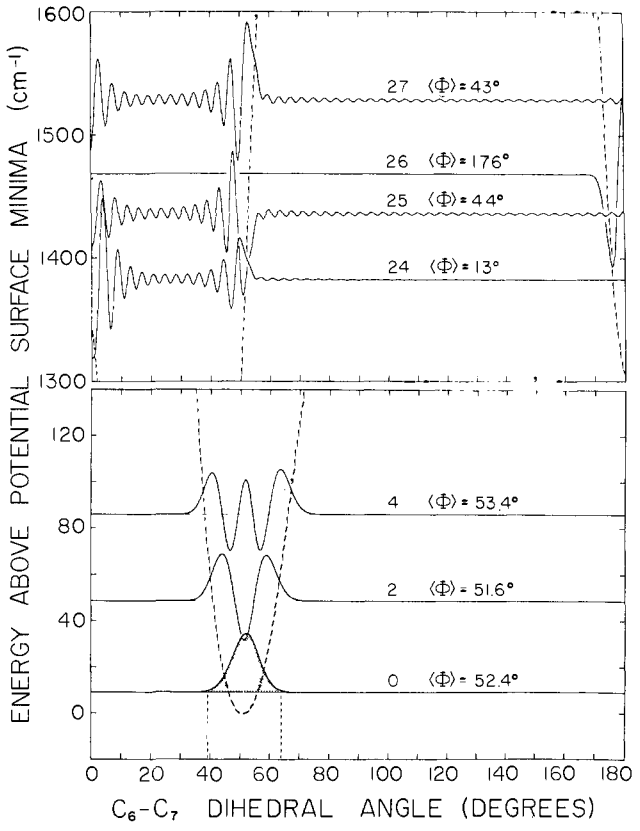

Figure 6. Selected low-lying vibrational wave functions in the ground state potential well (bottom) and selected Franck–Condon active vibrational wave functions in the $\pi\pi^*$ excited state manifold (top) plotted as a function of C_6–C_7 dihedral angle. The vibrational level ($v'' = 0, 2, 4$; $v' = 24, 25, 26, 27$) and the expectation value for $\Phi(5, 6, 7, 8)$ are shown above each wave function. The dashed lines represent the ground and $\pi\pi^*$ excited state surfaces and are plotted as a function of energy above the classical potential well minima. Note that in the excited state, two potential wells with minima at ~25° and 180° are present and at energies ~1300 cm^{-1} above the 25° minimum, the wave functions tend to localize in one, or the other, potential well. Those that localize in the 180° well (cf. $v' = 26$) are totally Franck–Condon inactive. The small oscillations of the $v' = 25$ and $v' = 27$ wave function in the $\Phi = 65$ and $\Phi = 180$ region are an artifact of incomplete convergence of the Fourier basis set. All of the eigenfunctions shown are *even* states and are degenerate or nearly degenerate with *odd* states having identical expectation values and Franck–Condon activities. The $\pi\pi^*$ excited state vibrational manifold shown in the upper section is equally applicable to the "$^1A_g{}^{*-}$" and "$^1B_u{}^{*+}$" states to within the accuracy of our theoretical analysis.

$2 \leftarrow 1$ transition is at 19 cm^{-1}). At 1.8 K, >99% of the molecules occupy the lowest (doubly degenerate) ground state vibrational level shown in Figure 6. An analysis of the calculated wave function indicates that ~77% of the molecules in the $v'' = 0$ level are confined to a relatively small range of C_6–C_7 dihedral angles [$\Phi(5,6,7,8) = 52.4 \pm 4°$]. This result suggests that horizontal inhomogeneity is not important at liquid helium temperatures. However, the vibronic intensity distribution analysis shown at the botton of Figure 7 indicates that significant spectral diffuseness is associated with the Franck–Condon activity of higher vibrational modes of the $\pi\pi^*$ ("$^1B_u{}^{*+}$") excited singlet state C_6–C_7 torsional manifold. The vibronic activity of the higher vibrational levels of the excited state surface is associated with the large shift in the C_6–C_7 potential well minimum upon excitation [$\langle\Phi\rangle(S_0, v'' = 0) = 51.7°$; $\langle\Phi\rangle$("$^1B_u{}^{*+}$", $v' = 0) = 32.3°$]. In particular, excited state vibrational levels between $v' = 20$ and $v' = 30$ are primarily responsible for the observed vibronic intensity (see Figure 6).

In summary, therefore, the calculations suggest that at very low temperature (1.8 K), the principal source of spectral diffuseness in the λ_{max} band of *all-trans* retinal is associated with C_6–C_7 torsional vertical inhomogeneity of the "$^1B_u{}^{*+}$" $\leftarrow S_0$ transition. The electronic origin of the vertical inhomogeneity

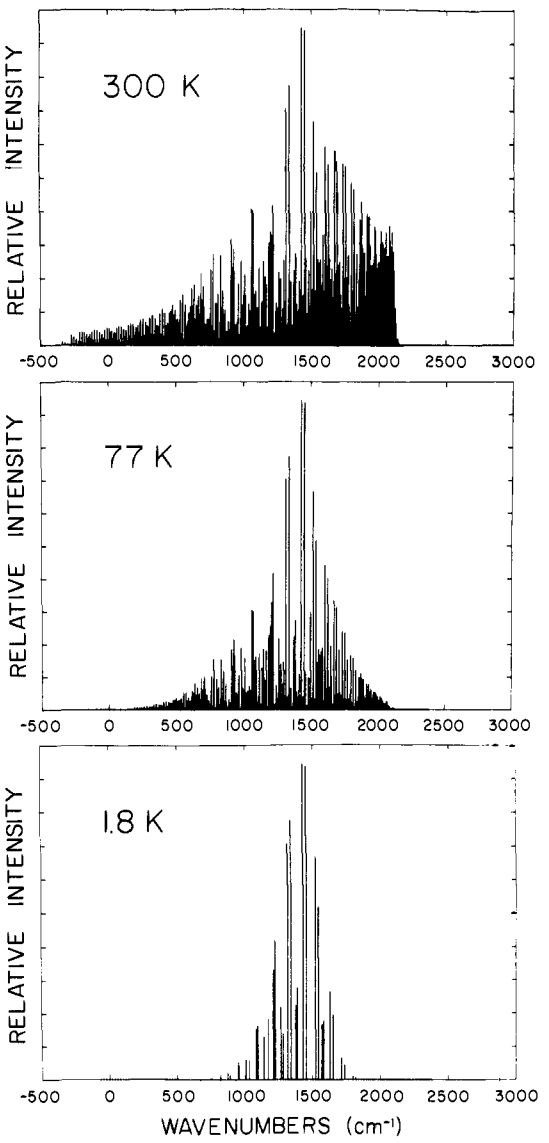

Figure 7. Distribution of vibronic activity in the "$^1B_u{}^{*+}$" $\leftarrow S_0$ transition for the C_6–C_7 torsional degree of freedom as a function of relative torsional energy and temperature. The transition energy is in wavenumbers relative to the system origin (i.e., 0 cm^{-1} corresponds to system origin, positive wave-numbers correspond to transitions at energies higher than the system origin).

is associated with partial C_6–C_7 bond-order reversal accompanying the $\pi^* \leftarrow \pi$ transition. The C_6–C_7 π-electron bond order is calculated (INDO-PSDCI) to increase from 0.241 to 0.292 upon excitation into the "$^1B_u{}^{*+}$" state.

1. Bond Order and the C_6–C_7 Torsional Potential Surface. A semiquantitative analysis of the bond-order effect can be carried out within the CNDO/2 approximation[21] by noting that the π-electron bond energy can be calculated using the expression

$$E_{\mu\nu} = 2P_{\mu\nu}\beta_{AB}S_{\mu\nu} - \tfrac{1}{2}P_{\mu\nu}{}^2\langle\mu\mu|\nu\nu\rangle + Z_AZ_BR_{AB}{}^{-1} + (P_{AA}P_{BB} - P_{AA}Z_B - P_{BB}Z_A)\langle\mu\mu|\nu\nu\rangle \quad (15)$$

where $P_{\mu\nu}$ is the bond order, β_{AB} is a semiempirical bonding parameter, $S_{\mu\nu}$ is the overlap integral, $\langle\mu\mu|\nu\nu\rangle$ is the two-center Coulomb repulsion integral, and the remaining terms have their usual definitions (ref 21). We assume μ references the $2p_\mu$ atomic orbital on atom A, and ν references the $2p_\pi$ atomic orbitals on atom B. The loss of $2p_\pi$–$2p_\pi$ bonding energy associated with torsional distortion can be approximated by

$$\Delta E_{\mu\nu}{}^{(\Delta\Phi)} = -[2P_{\mu\nu}{}^{(\Phi\to0)}\beta_{AB}S_{\mu\nu}{}^{(\Phi\to0)} - \tfrac{1}{2}[P_{\mu\nu}{}^{(\Phi\to0)}]^2\langle\mu\mu|\nu\nu\rangle][1 - \cos(\Phi)]^2 \quad (16)$$

Table I. Energies, Populations, Expectation Values, and Probability Distributions in the Low-Lying Vibrational Levels of the Ground State C_6–C_7 Torsional Potential Well

					P^f					
v'' [a]	E, cm^{-1} [b]	B [c]	ΣB [d]	$\langle\Phi\rangle$ [e]	$\langle\Phi\rangle \pm 1°$	$\langle\Phi\rangle \pm 2°$	$\langle\Phi\rangle \pm 4°$	$\langle\Phi\rangle \pm 8°$	$\langle\Phi\rangle \pm 16°$	$\langle\Phi\rangle \pm 32°$
0	11.6	0.084	0.084	52.4[g]	0.241	0.459	0.768	0.967	0.988	0.991
1	32.5	0.077	0.161	50.9	0.021	0.075	0.327	0.878	>0.999	>0.999
2	51.4	0.071	0.232	51.6	0.093	0.148	0.167	0.596	0.992	0.995
3	70.2	0.065	0.296	52.4	0.027	0.080	0.225	0.402	0.996	>0.999
4	89.0	0.059	0.356	53.4	0.025	0.077	0.194	0.358	0.969	0.996
6	127.2	0.050	0.460	54.7	0.018	0.074	0.155	0.342	0.814	0.997
8	165.3	0.042	0.547	56.2	0.047	0.056	0.137	0.268	0.693	0.997
10	201.5	0.035	0.620	58.3	0.014	0.064	0.101	0.226	0.555	0.997
13	253.3	0.027	0.708	59.5	0.028	0.047	0.109	0.202	0.465	>0.999
16	306.0	0.021	0.776	59.8	0.023	0.051	0.091	0.196	0.397	0.992
19	359.2	0.016	0.828	60.7	0.017	0.052	0.089	0.175	0.361	0.942

[a] Ground-state vibrational quantum number. [b] Vibrational energy in wavenumbers above potential well minimum. [c] Boltzmann population at 298 K (1 = 100%). [d] Boltzmann population of present level plus all levels lower in energy at 298 K. [e] Quantum mechanical expectation value for the C_6–C_7 dihedral angle (in degrees). [f] Probability of finding the C_6–C_7 dihedral angle with a value of $\langle\Phi\rangle$ plus or minus the specific angular deviation. For example, 24.1% of the molecules in the lowest vibrational level ($v'' = 0$) have dihedral angles in the range 51.4–53.4°. [g] The expectation value for Φ (52.4°) differs slightly from the potential energy minimum of the well (51.7°) because the potential surface is not symmetric.

where $P_{\mu\nu}^{(\Phi\to0)}$ and $S_{\mu\nu}^{(\Phi\to0)}$ are the bond order and overlap integral, respectively, evaluated at a reference dihedral angle of 0° or 180° (no torsional distortion) and Φ is the dihedral angle. Equation 16 is derived assuming a cos (Φ) dependence in both $P_{\mu\nu}$ and $S_{\mu\nu}$ and ignoring torsionally induced changes in all the other parameters. Accordingly, it is a very approximate relationship and is likely to overestimate the true energy of torsional distortion. The $2p_\pi$–$2p_\pi$ overlap integral for carbon atoms at $\Phi = 0°$ can be calculated using the expansion

$$S_{\mu\nu}^{(\Phi\to0)} = 1.3161 - 1.1173(R_{AB}) + 0.2514(R_{AB})^2 \qquad 1.2 < R_{AB} < 1.6 \quad (17)$$

R_{AB} is in angstroms. Equation 17 is accurate to three significant digits within the range 1.2–1.6 Å. An INDO-PSDCI calculation on a hypothetical geometry of *all-trans* retinal for $\Phi_{6,7} = 0°$ (planar 6-s-cis) predicts the following $C_6(2p_\pi)$–$C_7(2p_\pi)$ bond orders: $P_{\mu\nu}^{(\Phi\to0)} = 0.3848$ (S_0), 0.3455 ($n\pi^*$) 0.5428 ("$^1A_g{}^{*-}$"), 0.4809 ("$^1B_u{}^{*+}$"). The crystal geometry C_6–C_7 bond length is 1.48 Å [$S_{\mu\nu}^{(\Phi\to0)} = 0.213$, eq 17]. The other terms in eq 16 are $\beta_{AB} = -21$ eV and $\langle\mu\mu|\nu\nu\rangle = 10.3$ eV. At a reference dihedral angle of 50°, the following values for $\Delta E_{\mu\nu}^{(\Delta\Phi)}$ are obtained: 0.54 eV (S_0), 0.47 eV ($n\pi^*$), 0.81 eV ("$^1A_g{}^{*-}$"), 0.70 eV ("$^1B_u{}^{*+}$"). These values display a reverse trend relative to the potential energy minima for the C_6–C_7 torsional surfaces: 51.7° (S_0), 52.1° ($n\pi^*$), 23.8° ("$A_g{}^{*-}$"), 32.3° ("$^1B_u{}^{*+}$") [see Figure 4]. Equation 16 is therefore qualitatively useful in rationalizing the relative shifts in potential energy minima as a function of the calculated bond order.

2. Temperature Effect on Inhomogeneous Broadening. The vibrational levels in the ground state C_6–C_7 torsional well are very closely spaced (Table I). At ambient temperature, ~17% of the molecules are in vibrational levels above $v'' = 19$ roughly half of the molecules are in level $v'' = 6$ and below. We noted earlier that at 1.8 K, the C_6–C_7 torsional angle of *all-trans*-retinal is restricted to a relatively small range of dihedral angles (77% fall within $\Phi_{6,7} = 52.4 \pm 4°$). Higher vibrational levels, however, access a much greater range in $\Phi_{6,7}$ and at ambient temperature approximately 77% of the molecules will occupy dihedral angles of $54 \pm 16°$. The resultant vibronic intensity distribution shown at the top of Figure 7 is therefore a manifestation of horizontal inhomogeneity. Furthermore, a comparison of the 300 K and 1.8 K distributions (Figure 7) indicates that at ambient temperature, horizontal inhomogeneity dominates vertical inhomogeneity in producing spectral broadening. At 77 K, horizontal and vertical inhomogeneity are roughly of equal importance (Figure 7).

3. Comparisons with Previous Theoretical Calculations. Warshel and Karplus investigated inhomogeneous broadening in the vibronic spectrum of β-ionone, *all-trans*-retinal, and 11-*cis*-retinal with use of semiempirical consistent force field (QCFF) procedures.[6] Our theoretical methods differ significantly from those adopted in ref 6, and it is important to note that our observations are in substantial agreement with those presented by Warshel and Karplus. The QCFF method evaluates the vibronic spectrum with use of a harmonic basis set and the complete $3n$-dimensional space of the molecule. This approach will provide a better description of the low-lying torsional modes than our partial-adiabatic "one-dimensional" torsional model because the torsional modes tend to mix with skeletal wagging modes of the polyene chain. However, our "one-dimensional" model has included a significant (though not complete) degree of adiabatic minimization of the polyene chain atoms in constructing the potential surfaces for the C_6–C_7 torsional degree of freedom. Accordingly, a degree of skeletal motion is implicitly included in the torsional motion depicted in Figure 4. Furthermore, the multidimensional component of the torsional motion is implicitly included in the calculation of the vibrational levels because of the generality inherent in eq 6. Our methodology is therefore not "one dimensional" in the conventional sense because other degrees of freedom are included in generating the torsional surfaces and in calculating the kinetic energy of the torsional motion. However, a true molecular vibration does not follow adiabatic paths and to that extent our representation of the torsional vibronic manifolds are approximate.

The approximations that we have adopted are necessary in order to study the importance of anharmonicity on the vibronic spectrum. It should be emphasized that the QCFF procedures of ref 6 use a harmonic basis set which represents an approximation which we believe will incorrectly predict the intensity distribution function for transitions into higher vibrational levels of the torsional manifold of the "$^1B_u{}^{*+}$" excited state. Our calculations indicate that anharmonicity significantly influences the spacings of the higher vibrational levels (Figure 6) and this has a profound effect on the Franck–Condon intensity distribution.

The above mentioned differences in the present formalism and that used in ref 6 are therefore significant. Nonetheless, our conclusions are in substantial agreement with those presented by Warshel and Karplus. In particular, the inhomogeneous broadening observed in the electronic spectra of the visual chromophores is due in large part to vibronic effects ("vertical inhomogeneity"). Our calculations indicate that at 1.8 K, inhomogeneous broadening is almost entirely due to vibronic effects.

Warshel and Karplus also theoretically investigated the electronic spectrum of 11-*cis*-retinal and predicted that the $C_{11}{=}C_{12}$ torsion makes a significant contribution to the vibronic envelope although it is not as important as the C_6–C_7 torsion in generating inhomogeneous broadening in the 11-cis isomer.[6]

B. Rhodopsin. The λ_{max} absorption band of rhodopsin is broad and displays no hint of vibronic structure even at liquid helium

temperatures.[10,29,30] In contrast, the low-temperature absorption spectra of the protonated Schiff bases of *all-trans*- and 11-*cis*-retinal display distinct vibronic structure in the λ_{max} bands in the presence of excess anhydrous HCl.[20] The anhydrous HCl is presumed to electrostatically stabilize the positively charged carbon atoms and mimic the counterion environment of opsin.[20] The observed absorption maximum of the PSB + HCl/cage (77 K) is ~540 nm, similar to the absorption maximum of rhodopsin at 77 K (~505 nm). Recent studies suggest that two counterions are in close proximity to the chromophore in rhodopsin and are primarily responsible for producing the observed bathochromic shift of the pigment.[31,32]

The above observations lead to the following question: Why is the λ_{max} absorption band of rhodopsin broad and unstructured when a more (presumably) inhomogeneous solution environment yields a structured λ_{max} absorption band for the PSB + HCl complex? The following possibilities are evaluated: (a) The protein environment of opsin is more inhomogeneous than the solution environment. Accordingly, the spectral broadness of the rhodopsin absorption spectrum is due to a superposition of different spectra associated with slightly different opsin environments in the individual proteins. (b) Inhomogeneous broadening associated with the C_6–C_7 dihedral angle is sufficient to induce spectral diffuseness to a similar extent as observed in the visual chromophores. (c) The protein environment confines and/or distorts the chromophore thereby inducing vibronic activity in numerous vibrational modes that serve to annihilate distinct vibronic structure. (d) Vertical inhomogeneity is associated with a barrierless excited state potential surface for double bond isomerization. We propose that the latter mechanism may be the dominant source of inhomogeneous broadening in rhodopsin (and bacteriorhodopsin, see below). Before discussing this effect in detail, we will evaluate the other three mechanisms to show why they are less important.

The chromophore in rhodopsin is isolated in a hydrophobic pocket,[2] with an apparently distinct counterion environment.[31,32] Furthermore, it is believed that rhodopsin contains 50–60% α-helical structure and that the chromophore is located in the α-helical region (see ref 2 and references therein). Accordingly, the binding site of opsin is probably not significantly more inhomogeneous than a solution environment. We suggest that protein inhomogeneity will contribute to spectral diffuseness by increasing the "intrinsic" line width of the individual vibronic bands (~500 cm^{-1}, see below), but that protein inhomogeneity is not the primary source of the spectral diffuseness.

Four pieces of evidence suggest that mechanism b is of much less importance in spectral broadening of visual pigments than of retinal chromophores. First, as previously noted in the introduction, the presence of a β-ionylidene binding site in rhodopsin[12-14] will restrict both vertical and horizontal inhomogeneity. Second, charge redistribution in the π-electron system of the chromophore accompanying protonation of the Schiff base significantly decreases the magnitude of excitation induced C_6–C_7 $2p_\pi$–$2p_\pi$ bond order increase upon excitation. INDO-PSDCI calculations indicate that the π-electron C_6–C_7 bond order increases from 0.265 in the ground state to 0.278 in the "$^1B_u{}^{*+}$" $\pi\pi^*$ state. This difference is to be compared with that calculated for *all-trans*-retinal [0.242 (S_0) vs. 0.292 ("$^1B_u{}^{*+}$"), see section A.2]. Accordingly, the change in bond order upon excitation in the protonated Schiff base is insufficient to induce significant vertical inhomogeneity in the absorption spectrum. Third, the observation of distinct vibronic structure in the HCl/cage low-temperature absorption spectra of the protonated Schiff bases of *all-trans*- and 11-*cis*-retinal provides experimental evidence that inhomogeneous broadening is not intrinsic to the PSB chromophore. In fact, room temperature absorption spectra of retinal PSB chromophores display a "hint" of vibrational structure totally lacking in the retinal chromophores.[33] Fourth, artificial rhodopsin generated with use of 5,6-dihydroretinal (a chromophore which has vibronic structure in solution) exhibits complete inhomogenous broadening.[8a]

Table II. Energies, Vibrational Overlap Integrals, Expectation Values, and Probability Distributions for Various Vibrational Levels of the Lowest $\pi\pi^*$ Excited Singlet State C_{11}=C_{12} Torsional Potential Surface

				p^e		
v' [a]	E,[b] cm^{-1}	S^2 [c]	$\langle\Phi\rangle$ [d]	$\langle\Phi\rangle \pm 1°$	$\langle\Phi\rangle \pm 4°$	$\langle\Phi\rangle \pm 16°$
0	85.4	1.1 (−13)	89.3	0.3949	0.9523	0.9929
1	248.4	2.1 (−15)	89.2	0.0363	0.7734	>0.9999
2	405.8	1.0 (−14)	89.0	0.1466	0.4349	0.9960
10	1456	2.6 (−13)	84.3	0.0300	0.1457	0.8899
20	2309	1.7 (−12)	66.1	0.0362	0.1724	0.7802
30	2778	7.7 (−9)	46.2	0.0356	0.1016	0.4164
35	2945	0.0139	32.7	0.0084	0.0962	0.3890
36	2975	0.1272	26.8	0.0214	0.0793	0.3440
37	2999	0.3519	22.2	0.0057	0.0979	0.3468
38	3027	0.2370	28.2	0.0099	0.0927	0.3658
39	3062	0.1213	31.3	0.0290	0.1020	0.3802
40	3101	0.0656	33.4	0.0387	0.1068	0.3976
41	3143	0.0360	36.1	0.0113	0.0777	0.3794

[a] Excited state vibrational level. [b] Vibrational energy in wavenumbers above C_{11}=C_{12} excited state potential well minimum. [c] The square of the vibrational overlap integral between the lowest-lying ground state vibrational level and the indicated excited state vibrational level (i.e., $|\langle\Psi_{v'}(S_1)|\Psi_0(S_0)\rangle|^2$). Exponents (base 10) are given in parentheses. [d] Quantum mechanical expectation value for the C_{11}=C_{12} dihedral angle (*in* degrees, 0° = planar 11-cis). [e] Probability of finding the C_{11}=C_{12} dihedral angle with a value of $\langle\Phi\rangle$ plus or minus the specied angular deviation. For example, 39.5% of the molecules in the lowest excited singlet state vibrational level (v' = 0) have dihedral angles in the range 88.3–90.3°.

Mechanism c is difficult to evaluate because we have no specific information concerning the exact morphology of the binding site of opsin. However, the striking similarity between the resonance Raman spectra of the free PSB of 11-*cis*-retinal in solution and the chromophore in rhodopsin indicates that the opsin bound chromophore is not significantly distorted in the binding site and has a conformation very similar to that of the free chromophore in solution.[34-37] Furthermore, the λ_{max} position of the electronic absorption spectrum of rhodopsin can be fully rationalized without invoking chromophore distortion.[32]

We now demonstrate that a barrierless excited state potential surface for double bond isomerization [mechanism d] is sufficient unto itself for producing the spectral diffuseness observed in the λ_{max} band of rhodopsin.

Inhomogeneous Broadening and the Excited State Potential Surface for Double-Bond Isomerization. The primary photochemical event in the rhodopsin bleaching sequence is now recognized to involve an 11-cis to 11-trans photoisomerization (see ref 2 for a recent review). Bathorhodopsin (which contains a distorted all-trans chromophore[38-41]) is formed from rhodopsin (which contains an 11-cis chromophore) in less than 6 ps.[42,43] This

(29) Yoshizawa, T. In "Handbook of Sensory Physiology", Dartnall, H., Ed.; Springer-Verlag: Berlin, 1972; Vol. VII/1, pp 146–179.
(30) Yoshizawa, T.; Horiuchi, S. In "Biochemistry and Physiology of Visual Pigments", Lauger, H., Ed.; Springer-Verlag: Berlin, 1973; pp 69–81.
(31) Arnaboldi, M.; Motto, M. G.; Tsujimoto, K.; Balogh-Nair, V.; Nakanishi, K. *J. Am. Chem. Soc.* **1979**, *101*, 7082.
(32) Honig, B.; Dinur, V.; Nakanishi, K.; Balogh-Nair, V.; Gawinowica, M. A.; Arnaboldi, M.; Motto, M. G. *J. Am. Chem. Soc.* **1979**, *101*, 7084.
(33) Ishikawa, K.; Yoshihara, T.; Suzuki, H. *Waseda Daigaku Rikogaku Kenkyusho Hokoku* **1980**, *93*, 66.
(34) Mathies, R.; Freedman, T. B.; Stryer, L. *J. Mol. Biol.* **1977**, *109*, 367.
(35) Callender, R. H.; Doukas, A.; Crouch, R.; Nakanishi, K. *Biochemistry* **1976**, *15*, 1621.
(36) Cookingham, R. E.; Lewis, A. *J. Mol. Biol.* **1978**, *119*, 569.
(37) Cookingham, R. E.; Lewis, A.; Lemley, A. T. *Biochemistry* **1978**, *17*, 4699.
(38) Yoshizawa, T.; Wald, G. *Nature (London)* **1963**, *197*, 1279.
(39) Eyring, G.; Curry, B.; Mathies, R.; Broek, A.; Lugtenberg, J. *J. Am. Chem. Soc.* **1980**, *102*, 5390.
(40) Eyring, G.; Curry, B.; Mathies, R.; Fransen, R.; Palings, I.; Lugtenberg, J. *Biochemistry* **1980**, *19*, 2410.
(41) Birge, R. R.; Hubbard, L. M. *Biophys. J.* **1981**, *34*, 517.

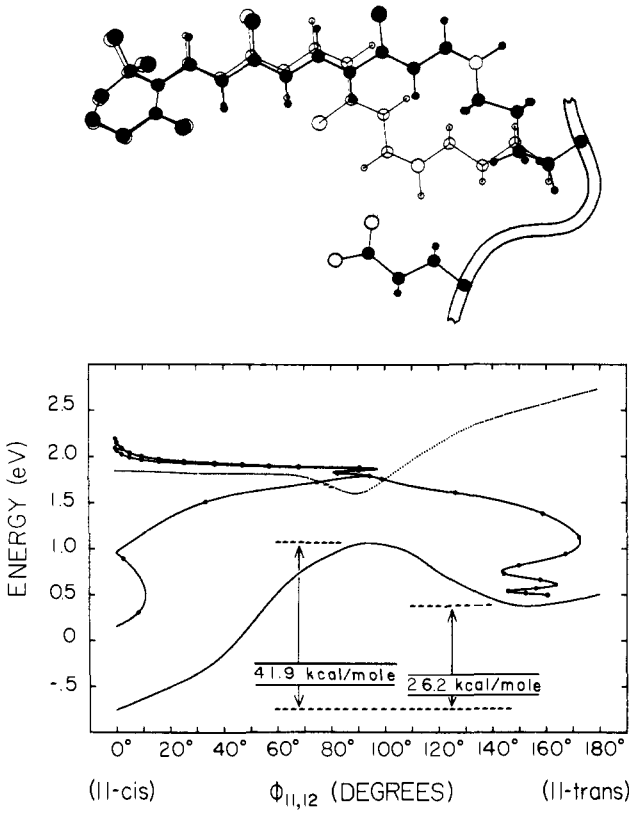

Figure 8. A simplified model of the active site of rhodopsin (top) and the resultant INDO-PSDCI surfaces in the ground and first excited singlet state as a function of the C_{11}=C_{12} dihedral angle (bottom). Trajectories associated with cis–trans isomerization in rhodopsin are shown in the bottom section. The excited state trajectory enters the activated complex in ~1.1 ps and oscillates with an average frequency of torsional motion of $\sim 4.5 \times 10^{12}$ Hz ($\sim$150 cm^{-1}). The lower left trajectory leads to the starting geometry (rhodopsin) in 1.8 ps; the lower right trajectory leads to isomerized product (bathorhodopsin) in 2.2 ps. These trajectories, along with the two torsional oscillations through $\Phi_{11,12}$ = 90° which precede them, are responsible for depleting the $S_1(\pi\pi^*)$ surface leaving a fraction of less than e^{-1} (0.37) of the molecules in the excited state. A quantum yield of 0.62 is calculated. The solid circles indicate trajectory increments of 0.1 ps. The two different excited state trajectories differ in excitation energy by 0.1 eV but coalesce before reaching the activated complex to produce wavelength-independent isomerization times and quantum yields. The lower left trajectory actually continues beyond the range of the horizontal axis to $\Phi_{11,12}$ = 11° but is shown reflected back toward positive dihedral angles for convenience. The cis–trans isomerization is accomplished without significantly disturbing the β-ionylidene ring. The counterion consists of the carboxylate group of a glutamic acid residue. One of the oxygen atoms of the carboxylate group is placed 3 Å (dotted lines) from the C_{15} carbon and the N_{16} imino nitrogen atoms. The ribbon connecting the lysine and glutamic acid residues schematically indicates that both residues are attached to the same protein backbone. These figures are adapted from ref 18 and 41 and the potential surfaces are used in the present paper to calculate the vibronic intensity distribution associated with a barrierless excited state potential surface for isomerization.

observation provides strong experimental support for the hypothesis that the photoisomerization procedes along a barrierless excited state C_{11}=C_{12} torsional potential surface.[2,18,43-48]

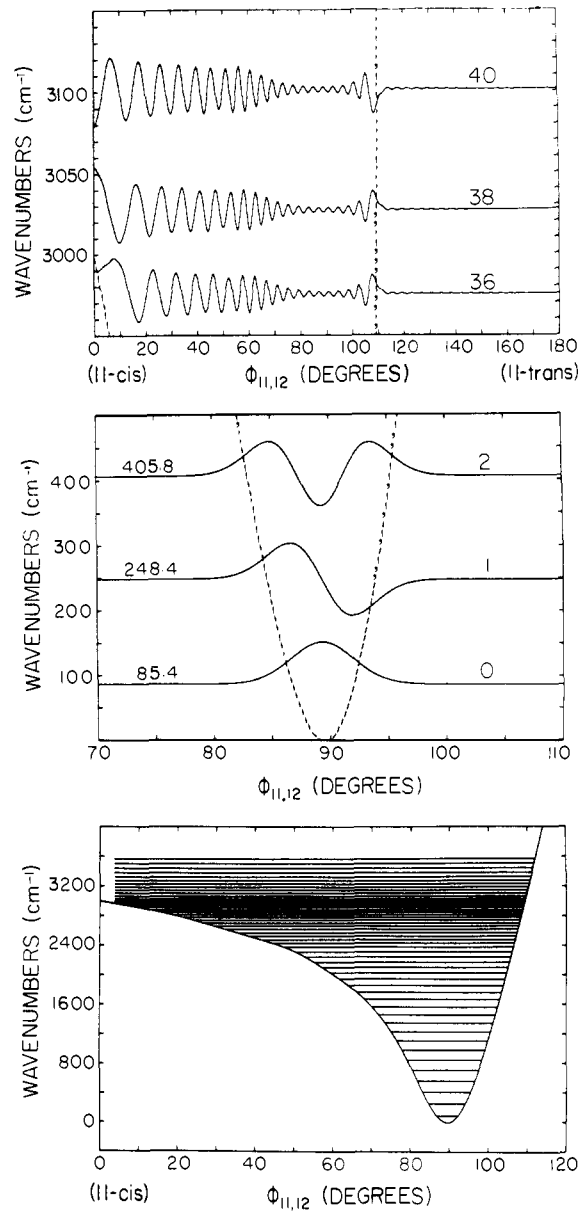

Figure 9. Selected wave functions in the first excited "$^1B_u^{*+}$" singlet state manifold associated with the C_{11}=C_{12} torsional potential surface of *all-trans-* (11-*cis*-) retinal. The excited state torsional potential surface was smoothed to permit Fourier transformation. The surface calculated using the expansion coefficients agrees with the corresponding INDO-PSDCI surface (Figure 8) to ±540 cm^{-1} or better. The first three levels (v' = 0, 1, and 2) shown in the middle graph are (to a first approximation) harmonic and completely Franck–Condon inactive. The levels shown in the top graph (v' = 36, 38, 40) are typical of the Franck–Condon active eigenfunctions and are highly anharmonic.

Birge and Hubbard have calculated the ground and excited state potential surfaces for the C_{11}=C_{12} torsional degree of freedom using the INDO-PSDCI procedures[19] and a single counterion model of the rhodopsin active site (Figure 8).[18,41] The details of the calculations have been described in previous papers (ref 18, 27, 41, and 47). The resulting (transformed) surface is shown in Figure 9 along with selected vibrational wave functions. The energies and salient properties of various vibrational levels in the excited state C_{11}=C_{12} potential well are presented in Table II. As can be seen by reference to Figure 9 and Table II, the excited state vibrational manifold is very anharmonic. The ground state C_{11}=C_{12} torsional manifold is characterized by large vibrational splittings relative to the excited state surface. The lowest four

(42) Busch, G. E.; Applebury, M. L.; Lamola, A.; Retzepis, P. M. *Proc. Natl. Acad. Sci. U.S.A.* **1972**, *69*, 2802.
(43) Green, B.; Monger, T.; Alfano, R.; Aton, B.; Callender, R. *Nature (London)* **1977**, *264*, 179.
(44) Honig, B.; Ebrey, T. G.; Callender, R. H.; Dinur, U.; Ottolenghi, M. *Proc. Natl. Acad. Sci. U.S.A.* **1979**, *76*, 2503.
(45) Hurley, J. B.; Ebrey, T. G.; Honig, B.; Ottolenghi, M. *Nature (London)* **1978**, *270*, 540.
(46) Warshel, A.; Weiss, R. M. *J. Am. Chem. Soc.* **1979**, *101*, 6131.
(47) Birge, R. R. In "Primary Events in Biology Probed by Ultrafast Laser Spectroscopy", Alfano, R. R., Ed.; Academic Press: New York, in press.
(48) Honig, B. In "Primary Events in Biology Probed by Ultrafast Laser Spectroscopy", Alfano, R. R., Ed.; Academic Press: New York, in press.

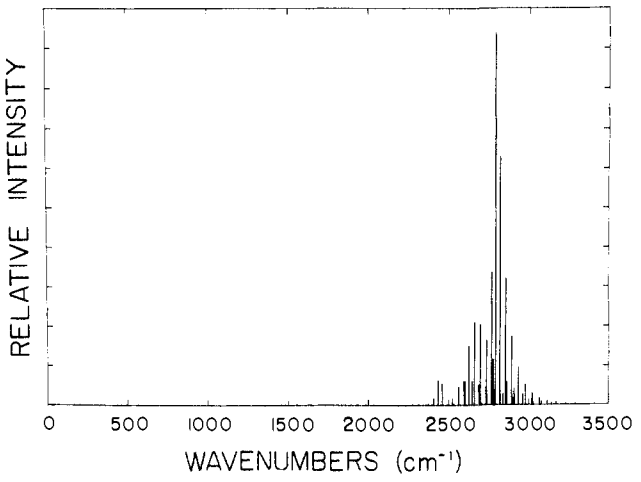

Figure 10. Distribution of vibronic activity in the "$^1B_u^{*+}$" ← S_0 transition for the C_{11}=C_{12} torsional degree of freedom as a function of transition energy relative to the system origin. The vast majority of the vibronic intensity is due to transitions originating from the ground vibrational level. Accordingly, the above intensity distribution is essentially temperature invariant. The most intense vibronic transition occurs at 2999 cm^{-1} and correspond to a $v' = 37 \leftarrow v'' = 0$ transition (see Table II). The square of the vibrational overlap integral ($(\langle\Psi'_{37}|\Psi''_0\rangle^2)$) is 0.3519, yielding an intensity ~50% greater than the strongest vibronic transition associated with the C_6–C_7 torsional surface (0.2358, see Figure 7). The integral inensity of the above vibronic progression is virtually identical with that associated with the 1.8 K, C_6–C_7 torsional progression (bottom of Figure 7).

vibrational level energies are 87.4 cm^{-1} ($v'' = 0$), 257.7 cm^{-1} ($v'' = 1$), 419.4 cm^{-1} ($v'' = 2$)8, 572.3 cm^{-1} ($v'' = 3$). The low-lying levels were fit to a quadratic function in v'' to yield the equation

$$E(cm^{-1}) = 87.38 + 174.78v'' - 4.3964(v'')^2 \qquad (18)$$

The ground state vibrational manifold is therefore relatively harmonic. At ambient temperature, ~53% of the molecules are in the lowest vibrational level. The calculated vibronic distribution at ambient temperature is shown in Figure 10. A calculation for a temperature of 1.8 K looks essentially identical (some of the weaker lines near the center of the distribution disappear). Accordingly, inhomogeneous broadening associated with the C_{11}=C_{12} double bond torsional potential surface is essentially invariant to temperature (1.8–300 K) and is entirely "vertical" (vibronic) in character. The extent of broadening due to the vibronic distribution shown in Figure 10 is comparable to that associated with the 1.8 K distribution shown in Figure 7 for the C_6–C_7 torsional surface of retinal. The calculated vibronic envelopes presented in Figures 11 and 12 serve to illustrate the above statement. We emphasize at the outset that these simulations are not intended to rigorously represent physical reality but are presented primarily to afford a comparison between the spectral broadening associated with C_6–C_7 torsional inhomogeneity vs. C_{11}=C_{12} torsional inhomogeneity. We used the vibrational levels and vibronic intensity distributions calculated by Warshel and Karplus for *all-trans*-retinal to represent the initial "vibronic basis set". The data were taken from Table VI of ref 6 with the restriction that only vibrational levels above 100 cm^{-1} were included along with their appropriate combination bands. We ignored vibrational levels below 100 cm^{-1} so that we would not include low-lying skeletal and torsional modes that might overlap in mode behavior with the 6–7 torsional progression (21 cm^{-1}; $1 \leftarrow 0$) modeled in the present paper. We used the same "vibronic basis set" for our simulations of the vibronic contour of rhodopsin even though this is clearly less appropriate. As previously stated, however, our primary goal is to compare the extent of spectral broadening associated with the C_6–C_7 and C_{11}=C_{12} torsional progressions; our use of the same "vibronic basis set" is therefore justified.

Two sets of contour simulations were calculated. The first set (Figure 11) was generated with the assumption of an intrinsic line width of 200 cm^{-1} [full width at half maximum (fwhm)]. This value is characteristic of a nearly homogeneous environment or a nonperturbing solvent. Were it possible to observe the spectrum of *all-trans*-retinal with use of Shpol'skii techniques, the contour simulations shown in Figure 11 suggest that a 1.8 K spectrum would reveal distinct vibronic structure. The simmulations shown in Figure 12 were generated with the assumption of an intrinsic line width of 500 cm^{-1}. This latter line width represents a more physically realistic value for the present systems. The analysis of Hemley and Kohler suggests that a value of ~550 cm^{-1} represents the limiting bandwidth (no β-ionylidene induced broadening) for the carotenoid polyenes at room temperature.[7a] Furthermore, the low-temperature (77 K) spectrum of anhydrovitamin A (Figure 3) exhibits a bandwidth of 530 cm^{-1} for the system origin (24 940 cm^{-1}) (compare Figures 12a and 3). Anhydrovitamin A represents an excellent reference molecule because the β-ionylidene ring is torsionally fixed and therefore will not generate inhomogeneous broadening of the vibronic spectrum. The contour simulations shown in Figure 12 predict that C_6–C_7 torsional inhomogeneity will completely remove the vibronic structure in the electronic spectrum of *all-trans*-retinal even at liquid helium temperatures (Figures 12d, 12e, and 12f). The calculated bandwidths of the broadened spectra are in good agreement with the experimental data on *all-trans*-retinal: $\Delta\tilde{\nu}_{calc}^{77\,K} = 4600$ cm^{-1} (Figure 12d), $\Delta\tilde{\nu}_{obsd}^{77\,K} = 4800$ cm^{-1} (EPA, Figure 1); $\Delta\tilde{\nu}_{cald}^{300\,K}$

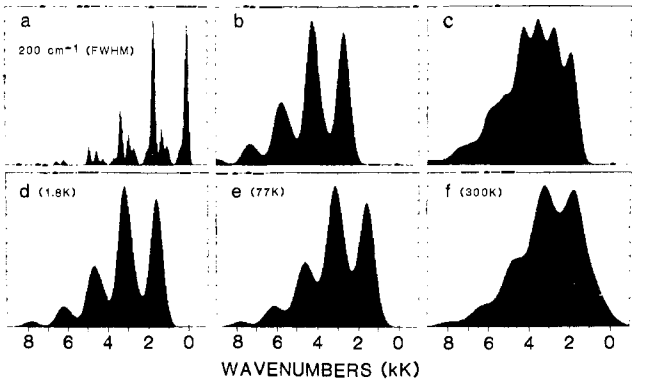

Figure 11. The effect of C_6–C_7 or C=C double-bond torsional inhomogeneity on the spectral contour of the hypothetical vibronic distribution is shown in spectrum a. An intrinsic line width of 200 cm^{-1} is assumed. Spectrum b is generated by including the vibronic distribution associated with the C_{11}=C_{12} torsional degree of freedom (Figure 10). Spectrum c is generated assuming two double bonds have barrierless excited state torsional potential surfaces with different energy well minima (see text). Spectra d, e, and f are generated by including the vibronic distributions associated with the C_6–C_7 torsional degree of freedom (Figure 7) for the three temperatures indicated. The energy axis is in wavenumbers (1 kK = 1000 cm^{-1}) above the system origin of the "vibronic basis set" shown in spectrum a.

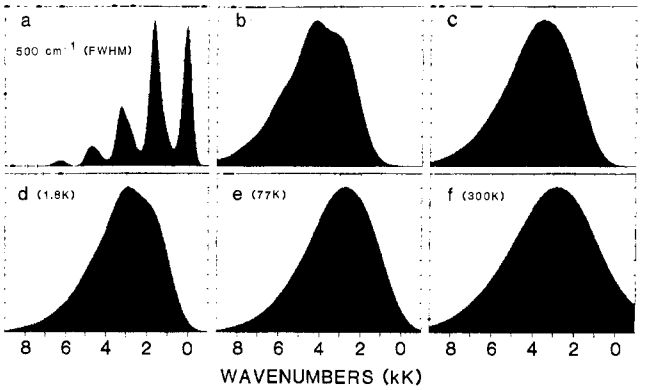

Figure 12. The effect of C_6–C_7 or C=C double bond torsional inhomogeneity on the spectral contour of the hypothetical vibronic distribution is shown in spectrum a. Details are identical with those described in the caption to Figure 11 with the exception that an intrinsic line width of 500 cm^{-1} is assumed.

= 5650 cm^{-1} (Figure 12f); $\Delta\bar{\nu}_{obsd}^{300\,K}$ = 5700 cm^{-1} (EPA). Two contour simulations for rhodopsin are shown in Figures 12b and 12c. The vibronic spectrum simulated in Figure 12b is constructed with the assumption that only one double bond (C_{11}=C_{12}) has a barrierless excited state potential surface for isomerization. The contour is generated with use of the vibronic progression shown in Figure 10 and is invariant to temperature (see previous discussions). The vibronic spectrum simulated in Figure 12c is constructed with the assumption that there are two double bonds with barrierless excited state potential surfaces for isomerization, one with a 3000 cm^{-1} potential well (Figure 9) and a second with a 2000 cm^{-1} potential well. Although there is no experimental or theoretical evidence to support the presence of two barrierless excited state potential surfaces for double bond isomerization in rhodopsin, there is compelling evidence to suggest that the all-trans chromophore in bathorhodopsin photochemically isomerizes to form rhodopsin (11-cis) or isorhodopsin (9-cis) along barrierless excited state surfaces.[2,41,44] The spectral simulation shown in Figure 12c suggests that two such surfaces, with slightly displaced barrier well minima, will enhance the extent of spectral diffuseness. A comparison of Figures 12b and 12d indicates that a single barrierless excited state potential surface for double bond isomerization will generate inhomogeneous broadening comparable to that predicted for C_6–C_7 torsional effects at liquid helium temperatures. This is the most important observation we wanted to illustrate in presenting these contour simulations. The electronic spectrum of *all-trans*-retinal remains diffuse down to 1.8 K.[3] We conclude that a barrierless excited state potential surface for double bond isomerization is sufficient to induce spectral diffuseness in the λ_{max} band of rhodopsin.

The observation that bathorhodopsin, lumirhodopsin, and metarhodopsin I all contain a protonated Schiff base chromophore[2] suggests that these bleaching sequence intermediates should also have barrierless lowest $\pi\pi^*$ excited state surfaces for double bond isomerization. Accordingly, these intermediates will also display a similar degree of vertical inhomogeneous broadening as predicted for rhodopsin. Metarhodopsin II, however, has an unprotonated Schiff base chromophore.[2] If the β-ionylidene ring of the chromophore in Meta II remains trapped in a restricted cleft, the absorption spectrum of Meta II should display at least a modest degree of vibronic structure at 77 K or below. Unfortunately, we have not found a low-temperature spectrum of Meta II in the literature to test this hypothesis.

C. Bacteriorhodopsin. Arguments similar to those presented for rhodopsin can be applied to spectral broadening of the λ_{max} band of bacteriorhodopsin. In this pigment system, however, the primary photochemical event is an all-*trans* (bR_{568}) to 13-cis (K_{610}) photochemical isomerization.[2,44,45,48-52] The primary event occurs on a picosecond time scale[53-55] and must therefore involve a barrierless 13-trans → 13-cis double bond isomerization.[2,44,45,48] This barrierless $\Phi_{13,14}$ excited state potential surface will therefore produce vertical inhomogeneous broadening in the λ_{max} absorption band of bacteriorhodopsin. Furthermore, the other photocycle intermediates containing PSB chromophores (K_{610}, L_{550}, N_{520}, O_{660})[2] should also exhibit vertical inhomogeneous broadening. In contrast, the M_{412} intermediate, which is presumed to contain an unprotonated SB chromophore,[2] should exhibit modest vibronic development in its low-temperature λ_{max} absorption band. A low-temperature (77 K) absorption spectrum of M_{412} has been reported by Becher et al.[11] and does in fact exhibit enhanced vibronic development relative to the other photocycle intermediates investigated (see Figure 7 of ref 11). Furthermore, the observation that the absorption spectrum of artificial (light adapted) bacteriorhodopsin generated from *all-trans*-5,6-dihydroretinal is broad and unstructured provides strong evidence that C_6–C_7 torsional inhomogeneity is not of significant importance in the spectral broadening of bR_{568}.[8b]

Acknowledgment. This work was supported in part by grants to R.R.B. from the National Institutes of Health (EY-02202) and the National Science Foundation (CHE-7916336), and to D.F.B. from the donors of the Petroleum Research Fund, administered by the American Chemical Society, and Research Corporation. R.R.B. thanks Professors R. L. Christensen, T. G. Ebrey, B. Honig, M. Karplus, B. E. Kohler, and A. Warshel for interesting and helpful discussions.

Registry No. *all-trans*-Retinal, 116-31-4; 9-*cis*-retinal, 514-85-2; 11-*cis*-retinal, 564-87-4; 13-*cis*-retinal, 472-86-6; anhydrovitamin A, 1224-78-8.

(49) Aton, B.; Doukas, A. G.; Callender, R. H.; Becher, B.; Ebrey, T. G. *Biochemistry* **1977**, *16*, 2995.
(50) Hurley, J. B.; Becher, B.; Ebrey, T. G. *Nature* (*London*) **1978**, *272*, 87.
(51) Schulten, K.; Tavan, P. *Nature* (*London*) **1978**, *272*, 85.
(52) Warshel, A. *Photochem. Photobiol.* **1979**, *30*, 285.
(53) Applebury, M. L.; Peters, K. S.; Rentzepis, P. M. *Biophys. J.* **1978**, *23*, 375.
(54) Ippen, E. P.; Shank, C. V.; Lewis, A.; Marcus, M. A. *Science* **1978**, *200*, 1279.
(55) Kaufman, K. T.; Rentzepis, P. M.; Stoeckenius, W.; Lewis, A. *Biochem. Biophys. Res. Commun.* **1976**, *68*,, 1109.